Westfälische Wilhelms-Universität Münster

IBB Institute for Biomagnetism and Biosignalanalysis

Applied Mathematics Münster

Sparse Recovery Conditions and Realistic Forward Modeling in EEG/MEG Source Reconstruction

Felix Lucka[1,2,3], Sina Tellen[1], Carsten H. Wolters[2,3], Martin Burger[1,3]

(1) Institute for Applied Mathematics (2) Institute for Biomagnetism and Biosignalanalysis (3) Cells in Motion Cluster of Excellence. All: University of Münster, Germany

Background: EEG/MEG Source Reconstruction

Measuring the induced electromagnetic fields at the head surface to estimate the instantaneous, underlying, activity-related ion currents in the brain (*instantaneous/static EEG/MEG source reconstruction*) is a challenging, high-dimensional, severely ill-posed inverse problem:

$$\text{(IP)} \quad Ax = b, \qquad b \in \mathbb{R}^m,\ x \in \mathbb{R}^n,\ A \in \mathbb{R}^{m \times n}$$

where b represents the measured data at 74 EEG or 273 MEG sensors (Figure 1), x represents the amplitudes of the discretized current field at n source locations distributed in the gray matter (Figure 4) oriented in normal direction of the cortical surface (*normal constraint*). A common source density is $n \approx 8000$. Computing the system matrix A requires constructing a model of the head's tissues (*head model, see* Figure 2,3) and solving the underlying PDEs on it (*forward computation*).

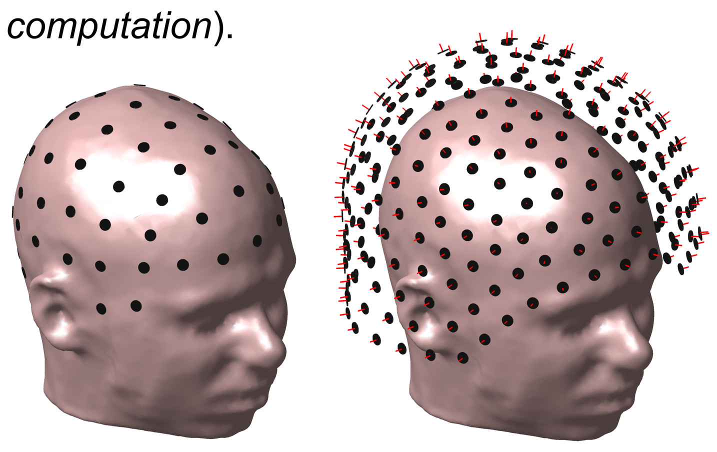

Figure 1: EEG (left) and MEG (right) sensors.

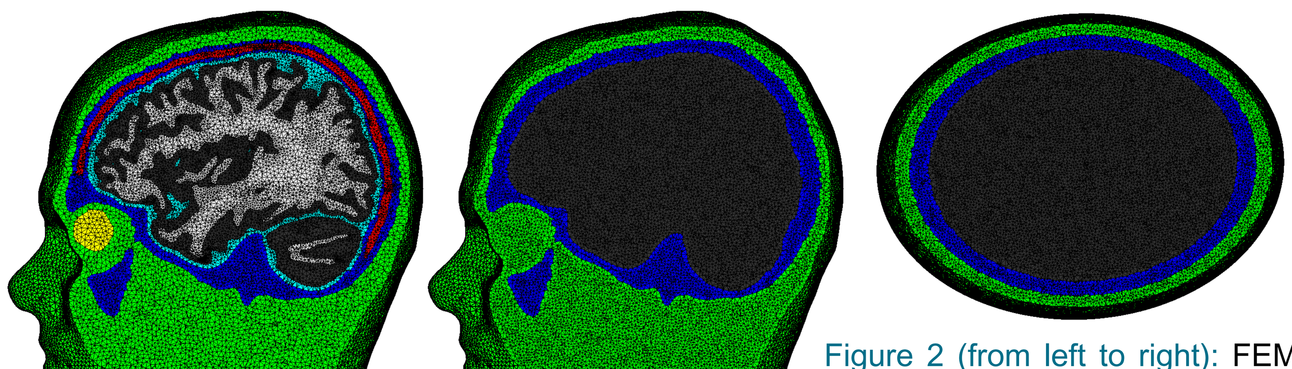

Figure 2 (from left to right): FEM head models HM1, HM2 and HM3 reflecting various degrees of realism used to model the geometry and tissue conductivity of the head of a patient. See Tellen, 2013 for a detailed description of the model generation.

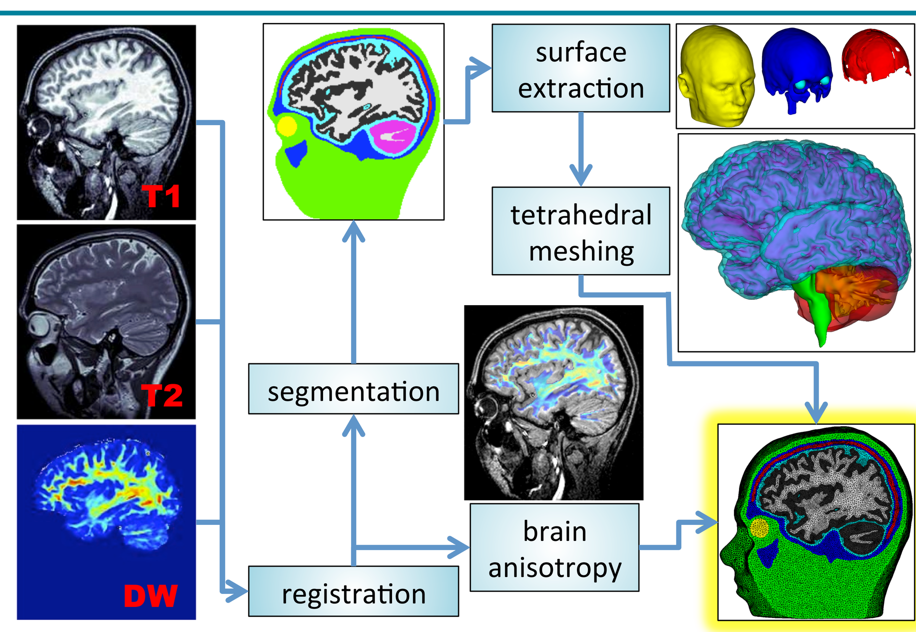

Figure 3: Procedure to build an individual, realistic, anisotropic finite element (FE) head model. Compartments: Skin, eyes, skull compacta, skull spongiosa, csf, gray and white matter of both cerebrum and cerebellum and brain stem. For gray and white matter, anisotropic conductivities are used, which have been computed from diffusion weighted MRI (DW-MRI) scans. A detailed description is given in Tellen, 2013 and the refereces therein.

Figure 4: n = 8000 discrete sources (black cones) visualized on a corresponding partition of the gray-white-matter interface. See Tellen, 2013 for a detailed description of the source space generation.

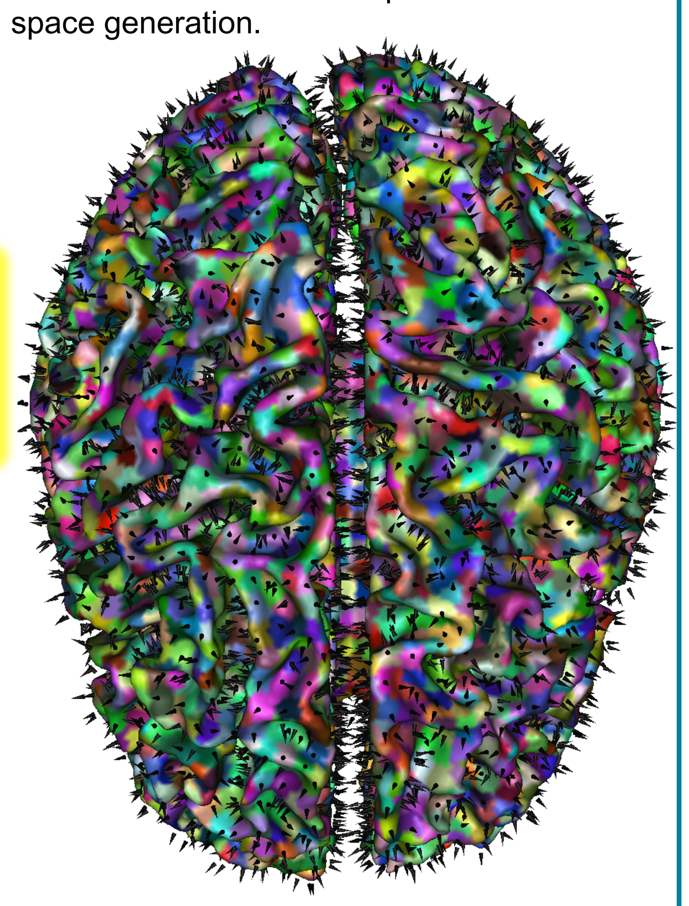

Motivation

Using spatial sparsity to solve (IP) has become popular in EEG/MEG (e.g., Lucka et al, 2012, Gramfort et al., 2013).

We are especially interested in the **interplay of realistic forward and sparse inverse modeling**

- Focus on how the intrinsic recovery properties of A evolve with modeling complexity (not on modeling errors!)
- Examined for l_2-norm but not for l_1-, l_{21}-norm or *hierarchical Bayesian modeling* approaches (Lucka et al, 2012).
- Dependence on source density n: Spatial resolution of sparse EEG/MEG?
- Main problems: Source separation and localization.
- Suitable framework/tools for our examinations? Concepts from *compressed sensing*?

n	HM1	HM2	HM3
62	0,9569689	0,9637311	0,9468869
125	0,9889984	0,9699115	0,9774069
250	0,9960846	0,9912376	0,9941620
500	0,9946813	0,9954526	0,9964294
1000	0,9995217	0,9989610	0,9982496
2000	0,9997652	0,9989881	0,9990561
4000	0,9999959	0,9999998	0,9999992
8000	**0,9998974**	**0,9999712**	**0,9999455**

Table 1: Coherence of the EEG system matrix A.

n	HM1	HM2	HM3
62	0,9569689	0,9637311	0,9468869
125	0,9889984	0,9699115	0,9774069
250	0,9960846	0,9912376	0,9941620
500	0,9946813	0,9954526	0,9964294
1000	0,9995217	0,9989610	0,9982494
2000	0,9997649	0,9988619	0,9990548
4000	0,9999068	0,9999705	0,9999447
8000	**0,9996511**	**0,9999274**	**0,9999016**

Table 2: Lower bound to δ_2 by Monte Carlo simulation.

Uniform and Nonuniform Recovery Conditions

We want to recover the k-sparse solution x_0 (support set I) of

$$\text{(L0)} \quad \min |x|_0 \quad s.t. \quad Ax = b$$

from the solution x_1 of

$$\text{(L1)} \quad \min \|x\|_1 \quad s.t. \quad Ax = b$$

Uniform recovery conditions guarantee the recovery of *all* k-sparse x_0. The strongest relies on the *coherence* of A:

$$\text{(Cho)} \quad k \leqslant \tfrac{1}{2}(\mu^{-1} + 1); \qquad \mu = \max_{i \neq j} |a_i^T a_j|$$

Weaker conditions rely on the *restricted isometry* constant of A, i.e., the smallest number δ_k s.t.:

$$\text{(RIP)} \quad (1 - \delta_k)\|x\|_2^2 \leqslant \|Ax\|_2^2 \leqslant (1 + \delta_k)\|x\|_2^2$$

Nonuniform recovery conditions guarantee the recovery a particular x_0. Tropp, 2004 introduced

$$\text{(Tr04)} \quad \|A_I^+ a_j\|_1 < 1 \quad \forall\, j \notin I$$

while Fuchs, 2004 introduced the stronger conditions

$$\text{(Fu04a)} \quad |d_I^T a_j| < 1 \quad \forall\, j \notin I \text{ with } d_I = (A_I^T)^+ \text{sign}(x_I)$$

$$\text{(Fu04b)} \quad |d_I^T a_j| < 1 \quad \forall\, j \notin I \text{ with } d_I \ s.t.\ A_I^T d_I = \text{sign}(x_I)$$

(Fu04b) is also known as a *dual certificate* or strong *source condition* (Möller, 2012):

$$\text{(SSC)} \quad \exists\, p \in \partial\|x\|_1 \quad s.t. \quad p \in range(A^T), \quad \|p_{I^c}\|_\infty < 1$$

Apart from its exact recovery guarantee, it also yields convergence rates and error estimates (e.g., Benning 2011).

The order between the conditions is given as

$$\text{(Cho)} \Rightarrow \text{(Tr04)} \Rightarrow \text{(Fu04a)} \Rightarrow \text{(Fu04b)} \Leftrightarrow \text{(SSC)}$$

n	HM1	HM2	HM3
62	0,059	0,195	0,098
125	0,029	0,090	0,035
250	0,005	0,017	0,002
500	0	0,004	0
1000	0	0,001	0
2000	0	0	0
4000	0	0	0
8000	**0**	**0**	**0**

n	HM1	HM2	HM3
62	0,181	0,359	0,225
125	0,105	0,224	0,143
250	0,053	0,104	0,061
500	0,023	0,050	0,034
1000	0,013	0,022	0,014
2000	0,010	0,012	0,006
4000	0,003	0,006	0,002
8000	**0,001**	**0,003**	**0,003**

n	HM1	HM2	HM3
62	1	1	1
125	1	1	1
250	0,975	0,978	0,972
500	0,929	0,948	0,931
1000	0,879	0,905	0,882
2000	0,795	0,821	0,787
4000	0,712	0,762	0,712
8000	**0,660**	**0,677**	**0,629**

Table 3: Empirical probability of (Tr04) (left), (Fu04a) (middle) and (Fu04b)/(SSC) (right) being true for k = 2 and N = 2000 samples.

Preliminary Results

Restriction to 3 head models, max n = 8000, EEG, scalar reconstruction.

- Table 1 shows the coherence of A which also upper-bounds δ_2. Table 2 shows lower bounds for δ_2 from extensive Monte Carlo simulations. For practical n (≥ 1000) both are extremely close to 1 and, thus, don't provide any recovery guarantees.
- Table 3 shows the empirical probabilities of the nonuniform conditions being true for k = 2 and N = 2000 samples. As expected, the likelihood rises from (Tr04) to (Fu04b)/(SSC).
- The gap between (Fu04a) and (Fu04b)/(SSC) is dramatic. Trends in (Fu04a) are not predictive of trends in (Fu04b)/(SSC).
- Results for MEG, other head models and/or for k = 3 confirm the results presented here.
- As expected, all guarantees degrade as the source density n increases.

Conclusions

- For system matrices A from severely ill-posed inverse problems like EEG/MEG, conditions (Cho), (RIP), (Fu04a) might be too strong, especially for a dense discretization.
- (Fu04b)/(SSC) are more difficult to compute, but may provide promising tools to analyze sparse recovery properties. In addition, they provide convergence rates and error estimates and extend to more general regularization like (generalized) total variation (Benning, 2011, Möller, 2012) which have also been considered for EEG/MEG (Haufe et al., 2008, Gramfort et al., 2013).
- Note that we addressed spatial inversion only. Our results do not extend to temporal decoding in EEG/MEG!

Extensions and Outlook

- Going from normal constraint to vector reconstruction leads to *block sparsity* (see Haufe et al., 2008, Tellen, 2013).
- Neurophysiologically plausible source orientation constraints.
- Column-normalization is ambivalent in l_2-norm approaches, situation for sparse inversion is not examined up to now.
- Computation of (Fu04b)/(SSC) needs to be improved.
- Methodology needs to target clinically relevant questions to be meaningful in practice.
- Practical definition of the spatial resolution of sparse EEG/MEG inversion?
- Examine EEG-MEG combination from a sparse inversion perspective.
- Incorporate noise, artifacts and non-sparse background activity

References

Benning M, 2011. *Singular Regularization of Inverse Problems*. PhD Thesis, University of Muenster, Germany.

Fuchs JJ, 2004. *On sparse representations in arbitrary redundant bases*. IEEE Trans Inf Theory 50(6).

Gramfort A, Strohmeier D, Haueisen J, Hämäläinen MS, Kowalski M. *Time-frequency mixed-norm estimates: Sparse M/EEG imaging with non-stationary source activations*. NeuroImage 70(0).

Haufe S, Vadim NV, Ziehe A, Müller KR, Nolte G, 2008. *Combining sparsity and rotational invariance in EEG/MEG source reconstruction*. NeuroImage 42(2).

Möller M, 2012. *Multiscale Methods for Generalized Sparse Recovery and Applications in High Dimensional Imaging*. PhD Thesis, University of Muenster, Germany.

Lucka F, Pursiainen S, Burger M, Wolters CH, 2012. *Hierarchical Bayesian Inference for the EEG Inverse Problem using Realistic FE Head Models: Depth Localization and Source Separation for Focal Primary Currents.* Neuroimage 61(4).

Tellen S, 2013. *Sparse Reconstruction and Realistic Head Modeling in EEG/MEG*. Master thesis, University of Muenster, Germany.

Tropp JA, 2004. *Greed is good: algorithmic results for sparse approximation*. IEEE Trans Inf Theory 50(10).

living.knowledge WWU Münster

Cells in Motion Cluster of Excellence

volume visualization was done with:

Corresponding author:

Felix Lucka

✉ felix.lucka@wwu.de